Proceedings of ASME Turbo Expo 2011
GT2011
June 6-10, 2011, Vancouver, British Columbia, Canada

GT2011-46080

FORCED FLAME RESPONSE OF A LEAN PREMIXED MULTI-NOZZLE CAN COMBUSTOR

Michael T. Szedlmayer, Bryan D. Quay, Janith Samarasinghe, Alex De Rosa,
Jong Guen Lee and Domenic A. Santavicca
Center for Advanced Power Generation
The Pennsylvania State University, University Park, PA, 16802

ABSTRACT

An experimental investigation was conducted to determine the air-forced flame response of a five-nozzle, 250 kW, lean premixed gas turbine can combustor. Operating conditions were varied over a range of inlet temperatures, inlet velocities, and equivalence ratios, while the forcing frequency was varied from 100 to 450 Hz with constant normalized velocity fluctuations of approximately 5%. The response of the flame's rate of heat release to inlet velocity fluctuations is expressed in terms of the phase and gain of a flame transfer function. In addition, chemiluminescence imaging is used to characterize the time-averaged and phase-averaged spatial distribution of the flame's heat release.

The resulting flame transfer functions and chemiluminescence flame images are compared to each other to determine the effects of varying the operating conditions. In addition, they are compared to data obtained from a single-nozzle combustor with the same injector.

The forced response of the multi-nozzle flame demonstrates a similar pattern to those obtained in a single-nozzle combustor with the same injector. An exception occurs at high frequency where the multi-nozzle flame responds to a greater degree than the single-nozzle flame. At low frequency the multi-nozzle flame dampens the perturbations while the single-nozzle flame amplifies them.

A number of minima and maxima occur at certain frequencies which correspond to the interference of two mechanisms. The frequency of these minima is nearly the same for the single-and multi-nozzle cases. When plotted with respect to Strouhal number instead of frequency there is a degree of collapse that occurs around the first observed minima.

INTRODUCTION

The generally accepted approach for meeting current and future NOx emissions regulations in land-based gas turbines is lean premixed combustion. Lean premixed gas turbine combustors, however, are more susceptible to combustion instabilities than conventional diffusion flame combustors.

Unstable combustion is the result of coupling between system acoustics and unsteady heat release, and the amplification of this process by feedback through one or more instability driving mechanisms. The resultant pressure and velocity fluctuations can cause large amplitude structural vibrations, increased heat fluxes at the system walls, flashback and flame blowoff. In the most extreme cases the outcome is catastrophic failure [1].

The process whereby fluctuations in the heat release rate produce pressure fluctuations is well understood; however, understanding the mechanisms whereby acoustic pressure and velocity fluctuations cause fluctuations in the rate of heat release remains an area of active research. To date there have been numerous flame response studies in single-nozzle research combustors which have provided valuable insights regarding the phenomenology of the flame's response [1-18]. These studies have identified a number of mechanisms which cause fluctuations in the flame's rate of heat release, including mean velocity fluctuations [1-5], vortex shedding [1, 3, 6-9], swirl fluctuations [10], equivalence ratio fluctuations [1, 3, 11, 12] and unsteady strain [13, 14]. Furthermore, many of these studies [2, 4, 10, 15-17] have yielded empirical and modeled flame transfer functions (FTF) which provide a quantitative relationship between the input perturbation, such as the velocity fluctuation, and the output perturbation, which is the fluctuation in the flame's rate of heat release [18].

Actual gas turbines, however, employ multiple nozzles, typically in an annular or can configuration. In a multi-nozzle combustor there are phenomena that are likely to affect the flame's response which are not accounted for by a single-nozzle flame transfer function. Perhaps the most important is the interaction between adjacent flames that occurs in a multi-nozzle combustor. This can be further complicated if there are differences in the flow conditions in each nozzle.

The flame response of multi-nozzle lean premixed gas turbine combustors has received little attention to date, with only four studies of annular combustors [19-22], and none of can combustors, reported in the literature.

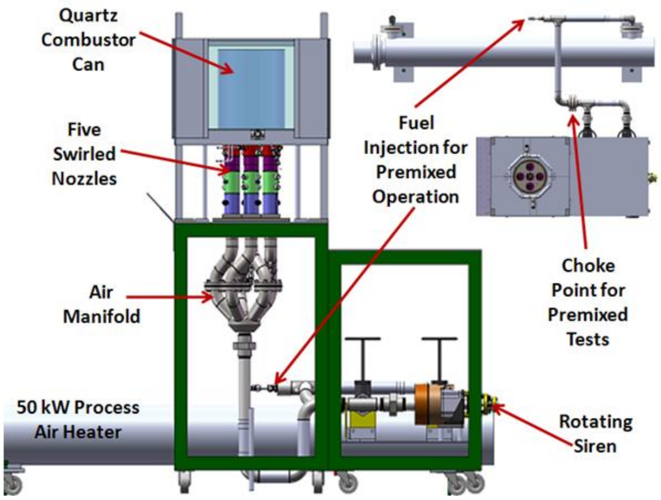

Figure 1: The Multi-Nozzle Combustor

Objectives

The objectives of this study are to experimentally determine the air-forced flame response of a multi-nozzle can combustor over a range of operating conditions and to compare the results to those previously obtained in a single-nozzle combustor using the same nozzle.

EXPERIMENTAL METHODS

Multi-Nozzle Can Combustor

The multi-nozzle can combustor test facility used in this study is illustrated schematically in figures **Error! Reference source not found.** and 2. Air is supplied at the required flow rate by an air compressor system capable of up to 600 SCFM at 300 psi. The flow rate to the combustor is controlled by a needle valve and monitored by a Sierra mass flow meter. The pressure at the meter is controlled by a Powreactor dome regulator. Downstream of the valve the air is preheated by a 50 kW process air heater to achieve the desired combustor inlet temperature. Downstream of the heater exit, natural gas fuel is injected transversely into the heated air through a multi-hole injector which was designed to achieve rapid mixing of the fuel and air. Additional mixing occurs as the fuel and air then flow through a 1.5" diameter pipe with an L/D of 15, as well as several elbows. At the end of this pipe, the fuel-air mixture flows through a choked orifice. The orifice has a diameter of .5" and the pressure drop across it is always a factor of two or greater. This ensures that the fuel injection and fuel-air mixing processes are not affected by pressure fluctuations downstream of the orifice and, as a result, the equivalence ratio entering the combustor is constant.

Downstream of the choked orifice, the premixed fuel and air enters a siren device that is used to produce periodic fluctuations in the velocity of the fuel-air mixture entering the combustor. The frequency of fluctuation is determined by the siren's rotational speed, while the amplitude of the fluctuation is controlled by varying the fraction of the fuel-air mixture that bypasses the siren.

Downstream of the siren the fuel-air mixture enters a manifold (Fig. 2) which divides the flow into five separate streams, one for each of the five nozzles in the multi-nozzle combustor. The manifold has been designed such that each of the five flow paths is geometrically identical. In addition, a perforated plate is installed in each leg of the manifold to help ensure that the flow to each nozzle is the same.

After exiting the manifold, the fuel-air mixture flows to each of the nozzles, which are connected directly to the combustor dump plane in a "four around one" configuration. The spacing of the nozzles relative to the diameter of the combustor can is typical of industrial can combustors. The nozzle tubes are ~2 inches in diameter and house a ~1 inch diameter centerbody and an axial swirler. The end of the centerbody is recessed ~1 inch from the face of the dump plane. The ratio of total nozzle area to the dump area is approximately 6 (dump ratio). The nozzles exit into the combustor can which is a 10 inch diameter, 12 inch long quartz cylinder. The downstream end of the quartz tube is unrestricted and open to the atmosphere. Consequently combustion takes place at atmospheric pressure.

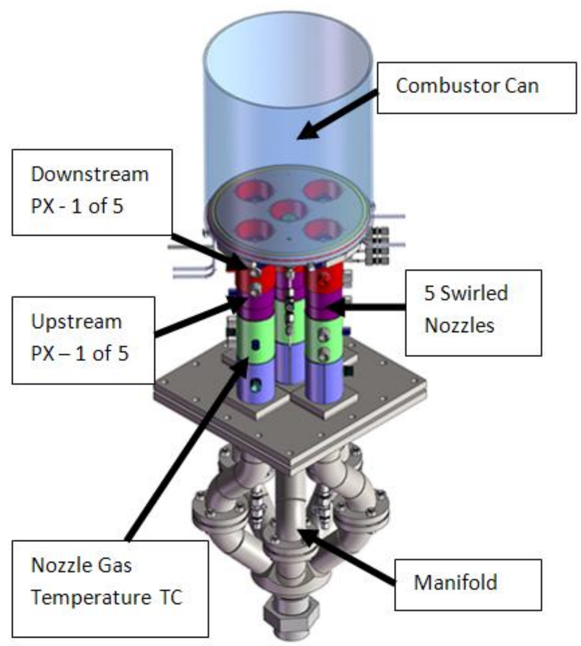

Figure 2: Can Combustor Close Up

Measurements

Electronic differential pressure gauges are used to measure the pressure drop across the swirler in each nozzle. Using empirical calibration data, the pressure drop across the swirler gives the velocity through the nozzle. The accuracy of this measurement is ±1 m/s. For the test conditions reported in this paper, the measured nozzle-to-nozzle variation in the mean velocity was less than ±2 m/s.

Thermocouples are used to measure the temperature of the fuel-air mixture approximately 1 inch upstream of the swirler in each of the nozzles. For the conditions tested, the nozzle-to-nozzle variation in the mixture temperature was less than 10˚C. The thermocouple in the middle nozzle serves as the control signal for the air heater.

Dynamic pressure measurements are made in each of the five nozzles at two locations between the swirler and the end of the centerbody, using water-cooled piezoelectric pressure transducers (PCB Model 112A22). They are referred to as the upstream and downstream pressure transducer (PX). The data acquisition system used for the pressure measurements has a sampling rate of 8192 Hz and provides a frequency resolution of 1 Hz. 32 data sets are obtained at each operating condition

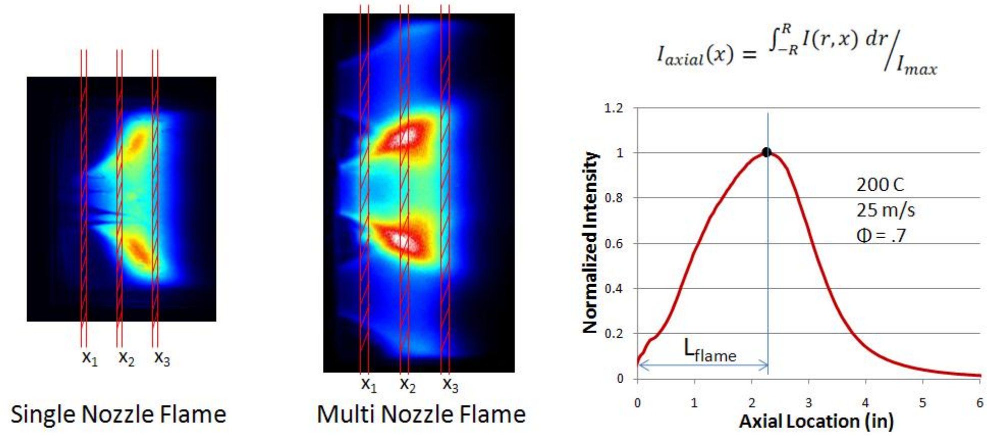

Figure 3: Axial Heat Release Flame Length Calculation Method, T_{inlet} = 200 C, V_{inlet} = 25 m/s, Φ = .7

to provide a statistically significant average and standard deviation.

The rate of heat release from the flame is determined from measurements of the CH* chemiluminescence intensity [23]. The total rate of heat release as a function of time is determined from measurements of the CH* emission from the whole flame using a 433 nm bandpass filter and a photo multiplier tube. The spatial distribution of the flame's rate of heat release is determined by imaging the CH* chemiluminescence emission onto an intensified CCD camera (Princeton Instruments #5768). The chemiluminescence images can be acquired as instantaneous, time-averaged or phase-averaged images.

Data Processing and Analysis

The dynamic pressure measurements in each nozzle are used as inputs to a two-microphone method (TMM) calculation [24]. The calculation provides the time varying velocity in each nozzle. At some conditions, particularly lower frequencies, the pressure signals exhibit a poor coherence, which results in an erroneous calculation of time varying velocity. Such data is discarded and not presented in the results.

The chemiluminescence signal from the PMTs is used to quantify the heat release from the flame as a function of time. By making use of a Fast Fourier Transform, the frequency domain of the signal can be determined. When the incoming flow is forced at a certain frequency a maximum appears in the fluctuation of the heat release rate at that frequency. This fluctuation is the result of the flame responding to the incoming perturbations through a number of feedback mechanisms. This will be discussed later. The amplitude and phase of the PMT signal at the forcing frequency are used as the output of the flame transfer function.

The flame transfer function (FTF) is the primary metric of most forced dynamics experiments. It is made up of two main components, a gain and a phase, and is a function of both forcing frequency (f) and amplitude (A). The phase of the FTF describes the phase difference between the input function and the output function at the forcing frequency. The phase of the FTF also represents the time required for the input perturbation to convect from the measurement location to the location in the flame where the perturbation results in a perturbation in the flame's rate of heat release. The gain relates the amplitude of the input, in this case, the velocity fluctuation (u'), to the output, here, the heat release rate fluctuation (Q'). There are 160 separate calculations of the input u' for each operating condition, 32 from each of the nozzles. Error bars on the FTF gain plots indicate 1 standard deviation of those 160 points. Any operating condition where the standard deviation is greater than 20% of the mean is discarded.

$$FTF(f,A) = \frac{\dfrac{Q'(f)}{Q_{mean}}}{\dfrac{u'(f)}{u_{mean}}} \qquad (1)$$

The flame length in the multi-nozzle combustor is determined from the chemiluminescence image of the unforced flame. Specifically, the flame length is defined as the distance from the end of the centerbody to the location of maximum rate of heat release in the axial heat release profile. For comparison with results from the single-nozzle combustor, this same method for determining the flame length is used. This method is illustrated for both the single-nozzle and multi-nozzle flames in Fig. 3.

RESULTS AND DISCUSSION

Operating conditions

All of the tests were performed at a combustor pressure of 1 atm, while the other operating parameters were varied over the range of values listed in Table 1. Forcing frequencies were selected based on past research that showed that the flame acts as a low pass filter [4], and that the gain drops off as the frequency increases. The forcing amplitude was selected to remain in the linear feedback range [16]. The linear regime refers to the range of forcing amplitudes where an increase in the input amplitude results in a proportional change in the output amplitude for a given frequency.

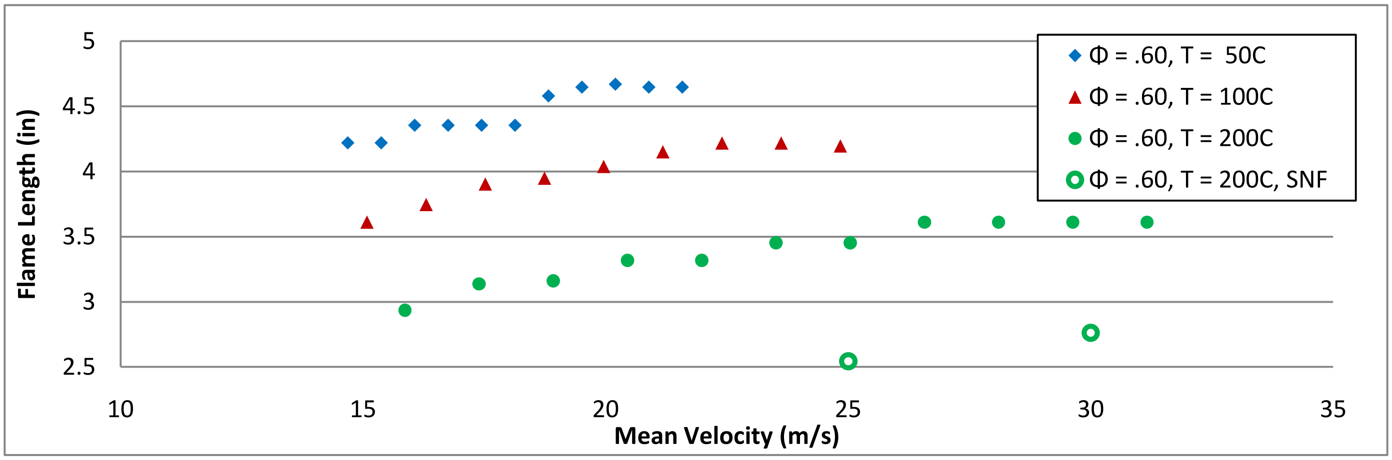

Figure 4: Multi-nozzle flame length for different inlet temperatures, and single-nozzle flame (SNF) length for a fixed inlet temperature

Table 1. Operating Conditions

Inlet Velocity (m/s) (u_{mean})	15-32
Equivalence Ratio	.5-.7
Inlet Temperature (°C)	50-200
Forcing amplitude (u'/ u_{mean})	5% - 15%
Forcing Frequency (Hz)	100-450

Stable Flame Length Comparison

Figures 4 and 5 show the flame length from the axial heat release method illustrated in figure 3. The axial flame length has been shown to have a direct relationship to the gain [2]. It will be used later in this study in the calculation of the Strouhal number.

Data at the same operating conditions from a single-nozzle experiment using the same nozzle are also shown on the figures. Single-nozzle data points have a white center. At the same operating condition the single-nozzle flame is shorter, but this most likely due, at least in part, to the increased dump ratio in the single-nozzle flame.

Figure 4 demonstrates the effect of inlet temperature on the flame length. As the inlet temperature increases, the flame length decreases. Similar behavior is observed when the equivalence ratio is increased as shown in figure 4. These effects have been observed in single-nozzle combustors [25] and are a result of the increased flame speed [26].

Note that for a given temperature and equivalence ratio the flame length appears to asymptote to a constant value at high velocities, even though the rate at which the flame consumes fuel continues to increase. It is also shown that the velocity at which this occurs decreases with decreasing temperature and equivalence ratio. In the flamelet regime [27], the total rate of fuel consumption is equal to the local fuel concentration times the local laminar flame speed integrated over the flame area. With fixed inlet temperature and equivalence ratio and neglecting flame stretch effects, the fuel concentration and the laminar flame speed are constant; therefore the total flame area must increase to consume the increased fuel flow rate at higher velocities. The flame area can increase by both an increase in the flame length and an increase in the turbulent wrinkling of the flame. These results suggest that initially the flame area increases as a result of increased flame length and increased turbulent wrinkling, however, there is a transition to where the flame length no longer increases and the increasing fuel consumption is entirely the result of increased wrinkling of the flame. It is

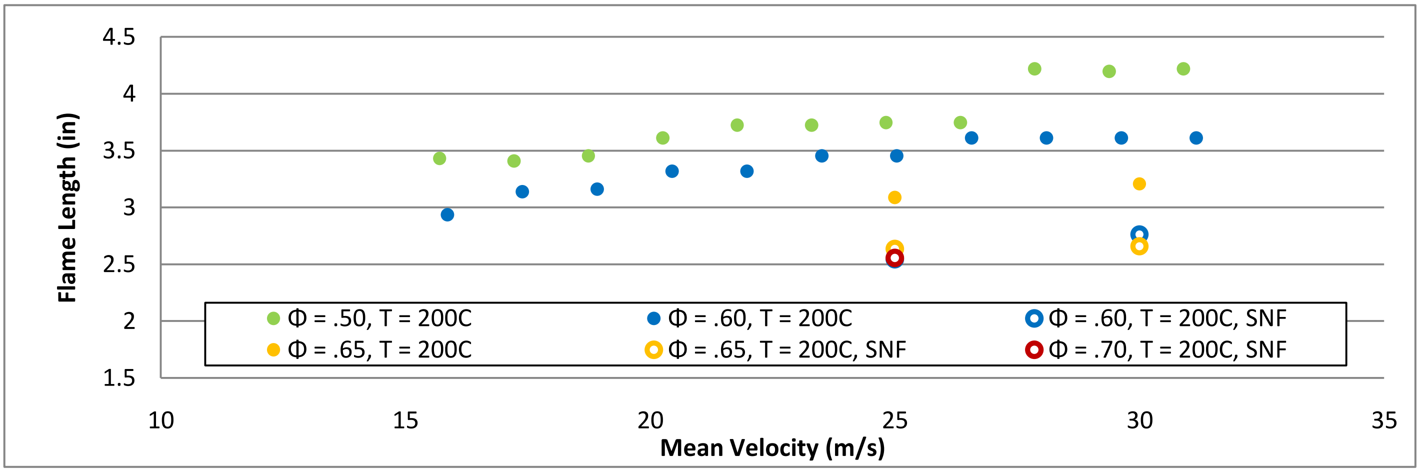

Figure 5: Flame length from Axial Heat Release for different equivalence, SNF denotes data from single nozzle flames

also possible that the increased rate of fuel consumption is associated with the flame interaction that occurs in the multi-nozzle combustor. In either case, this requires further study.

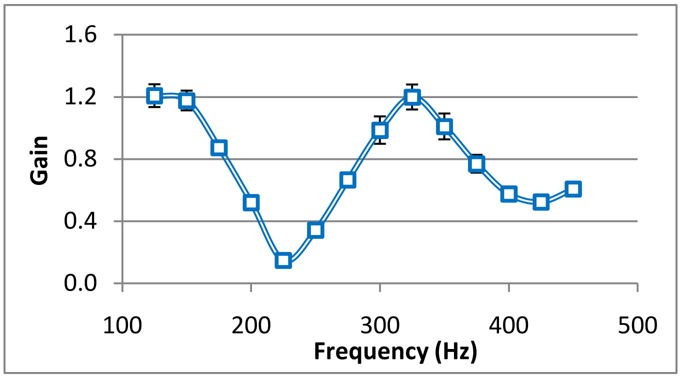

Figure 6: Flame Transfer Function Gain, T_{inlet} = 200C, u_{mean} = 25 m/s, Φ = .60, u' / u_{mean} = 5%

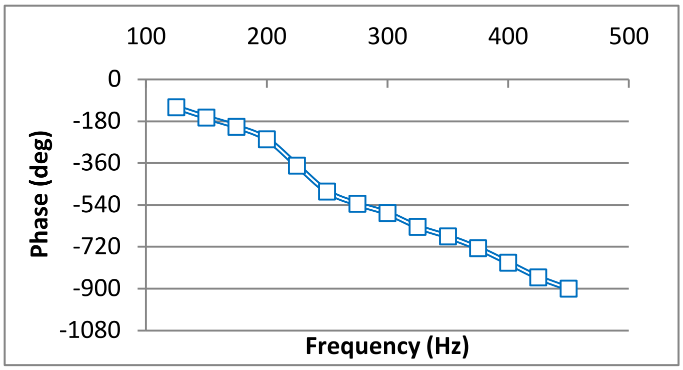

Figure 7: Flame Transfer Function Phase, T_{inlet} = 200C, u_{mean} = 25 m/s, Φ = .60, u' / u_{mean} = 5%

Flame Transfer Function

The flame transfer function (FTF) results from the multi-nozzle combustor are presented in figures 6 and 7 for u_{mean} = 25 m/s, T_{inlet} = 200 C and Φ = .6. These measurements were made with a normalized velocity fluctuation of 5% over a range of frequencies from 100 Hz to 450 Hz. The forcing amplitude was selected to remain in the linear regime.

In agreement with previous work [4, 10, 28], the gain of the FTF smoothly transitions through a number of maxima (150 Hz and 325 Hz in this case) and minima (225 Hz in this case). The extrema are thought to be the result of the interaction between two different coupling mechanisms. When the gain is at a maximum the mechanisms are in phase and interfere constructively, while when the gain is at a minimum the mechanisms are out of phase and interfere destructively.

Multi-Nozzle Flame Response at all Operating Conditions

Figure 8 shows the FTF for a 5% forcing amplitude at 4 different velocities at an equivalence ratio of .6 and inlet temperature of 200 C. Most notably there is little conformity between the various transfer functions, though there are obvious extrema. Previous work [16, 28] suggests that through use of the Strouhal number, FTFs for different operating conditions will collapse around the extrema. The Strouhal number is defined as:

$$St = \frac{L_{flame} * f_{forcing}}{u_{mean}} \qquad (2)$$

The Strouhal number takes into account a convective length scale of the flame. Using this definition of Strouhal number, the convection scale is based on the bulk flow velocity and the length of the flame. It is the amount of time it would take a perturbation to convect from the base of the flame at the centerbody to the center of heat release. The Strouhal number represents a ratio of this time scale to the period of forcing.

Figure 9 shows the same four FTFs presented in figure 8, but here they are plotted versus the Strouhal number. There is clearly a degree of collapse around the first observed minimum and maximum response frequency. This implies that the relative phase between the destructively interfering mechanisms is related to the convection time scale.

One of the most often cited coupling mechanisms is that of vortices shed from some geometric feature in the nozzle. They tend to be shed when a steep spatial gradient in the velocity convects past a step, such as the centerbody. The convection speed of this disturbance is known to be on the order of the bulk velocity. When the vortex interacts with the flame it will cause increased mixing between the hot products and the unburned reactants as well as an increased flame area, which will perturb the heat release.

The centerbody is known to be a source of these coherent structures, but it is also possible that they would be shed from the swirl vanes, or the outer edge of the nozzle. It is likely that at least one of the mechanisms involved in the feedback interference observed in figure 8 is vortex shedding. Because of all the possible locations for vortex shedding, the two mechanisms may actually both be vortices, or at least regions of high vorticity, shed from different locations.

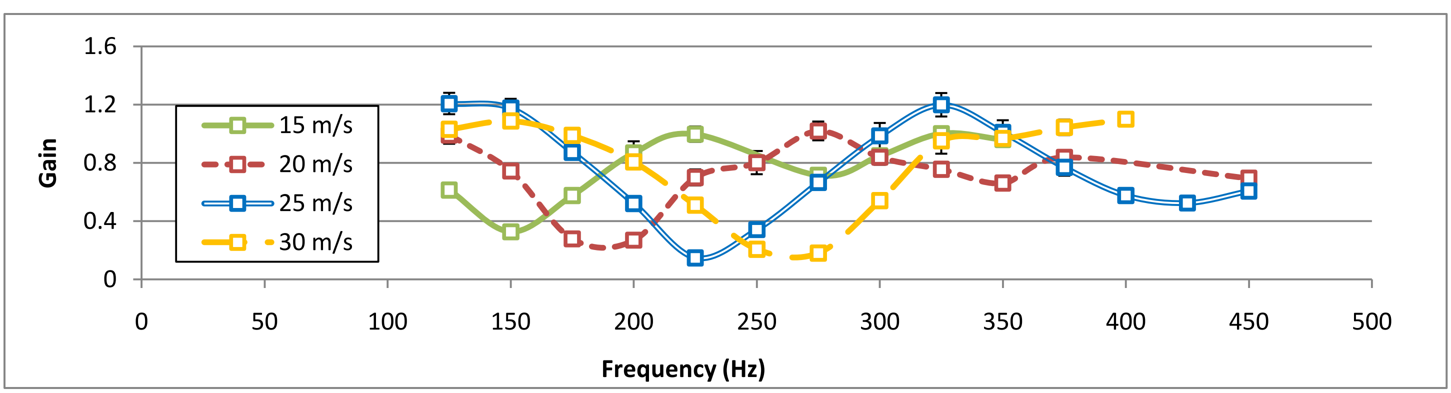

Figure 6: MNF FTFs for a range of velocities, T_{inlet} = 200C, Φ = .60, u' / u_{mean} = 5%

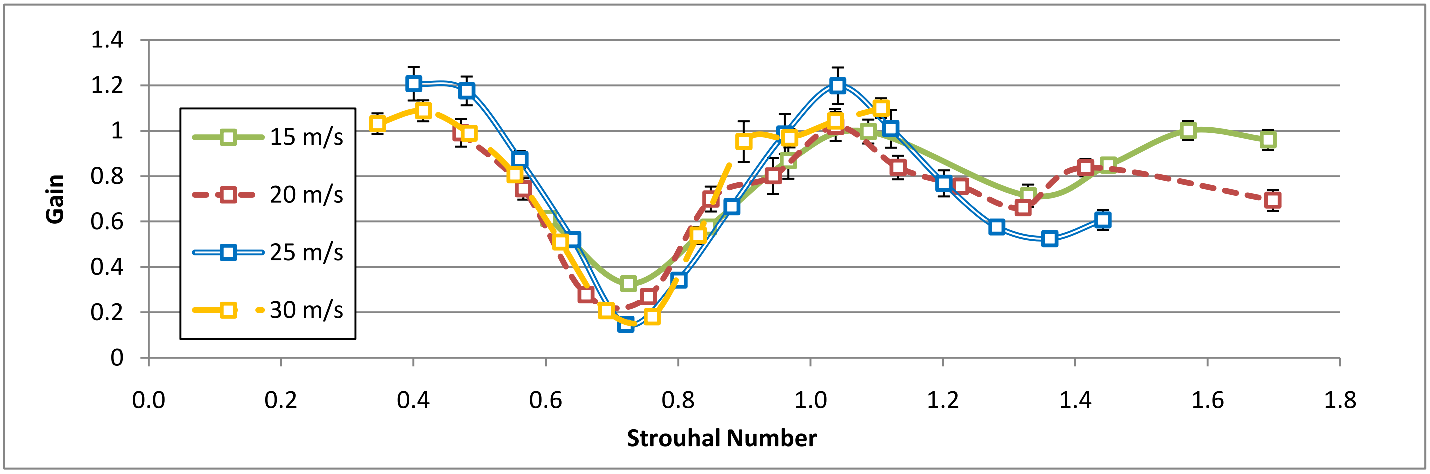

Figure 7: FTFs for a range of velocities plotted versus St, T_{inlet} = 200C, Φ = .60, u' / u_{mean} = 5%

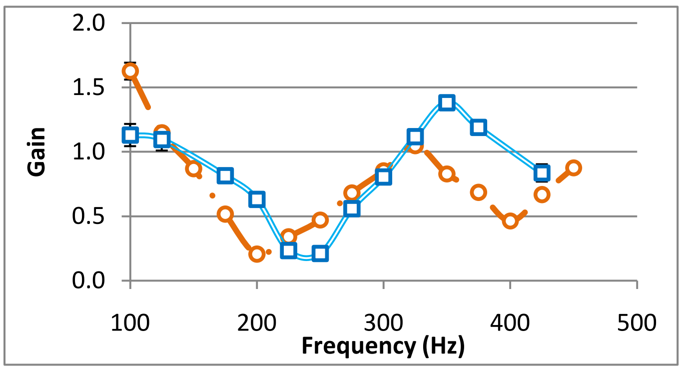

Figure 8: Multi nozzle to single nozzle FTF Gain comparison, u_{mean} = 30 m/s, T_{inlet} = 200C, Φ = .6

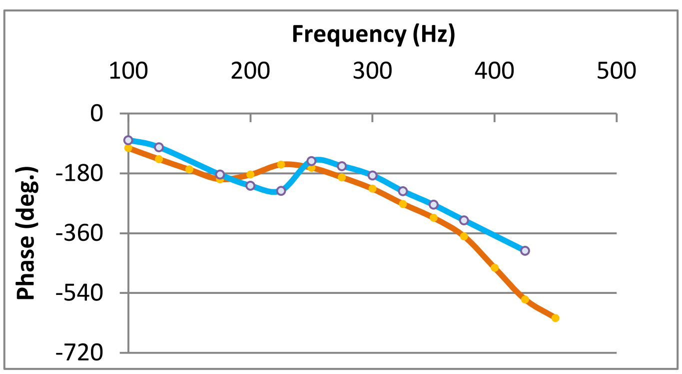

Figure 9: Multi nozzle to single nozzle FTF Phase comparison, u_{mean} = 30 m/s, T_{inlet} = 200C, Φ = .6

FTF comparison between Single-Nozzle and Multi-Nozzle

Figures 10 & 11 show the flame transfer function gain and phase of a multi-nozzle flame with a single-nozzle flame at the same operating conditions. The first minimum visible in figure 10 for the multi-nozzle configuration occurs around 25 Hz after the minimum for the single-nozzle. A similar shift occurs in the first observed maximum. This shifting behavior was observed between different inlet velocities in the previous section. This suggests that the addition of nozzles to the combustor changes the flame response in a manner similar to increasing the inlet velocity.

The low end of the frequency range suggests that single-nozzle flames respond more readily to low frequency perturbations. This is evidenced by the particularly high gain in the single-nozzle curve there.

At high frequencies, the response of the multi-nozzle and the single-nozzle flame is similar in pattern, although the multi-nozzle gain is higher. The higher the gain, the more potential an instability has to cause damage. Therefore, the higher frequencies, 300 Hz or more, require further investigation to determine if this elevated gain compared to single-nozzle flames is present at all operating conditions.

The phase data of the FTF also follows a similar pattern for single- and multi-nozzle flames. The two curves in figure 11 demonstrate an initially linear dependence on frequency, followed by a sudden jump that occurs at around 200 Hz. This frequency corresponds to the occurrence of the minimum in the gain data. From 200 Hz onward until 400 Hz both configurations' phases return to linear frequency dependence. At 400 Hz the single-nozzle phase is observed to experience another significant change in slope, corresponding to the second minimum of its gain curve. One possible explanation would be that as the phase of two mechanisms couple at the minimum a sudden change in the convective time scale occurs, which could be caused by a change in the flame length.

Phase Locked Imaging

Figures 12 & 13 each show a set of phase averaged images for two different forcing frequencies. Each image in these sets is averaged from 60 instantaneous images all at the same phase angle, each capturing 7.5 degrees of the 360 degree cycle. The two frequencies shown, 125 and 275 Hz, were selected to correspond to points of maximum response, as shown in figure 8. Note that figure 13, at 275 Hz, has an elevated forcing amplitude. Separate tests where the amplitude was varied showed that 15% remained in the linear regime, so the mechanisms causing the coupling should be the same and the gain should not change.

As one would expect, each set shows a smooth transition through high and low intensity flames as the flame responds to the fluctuating velocity. There is also a change in flame length, as shown in figure 14. The red line indicates the procession of the point of max heat release through the cycle. This is due to fluctuating mass flow, as in the unforced case.

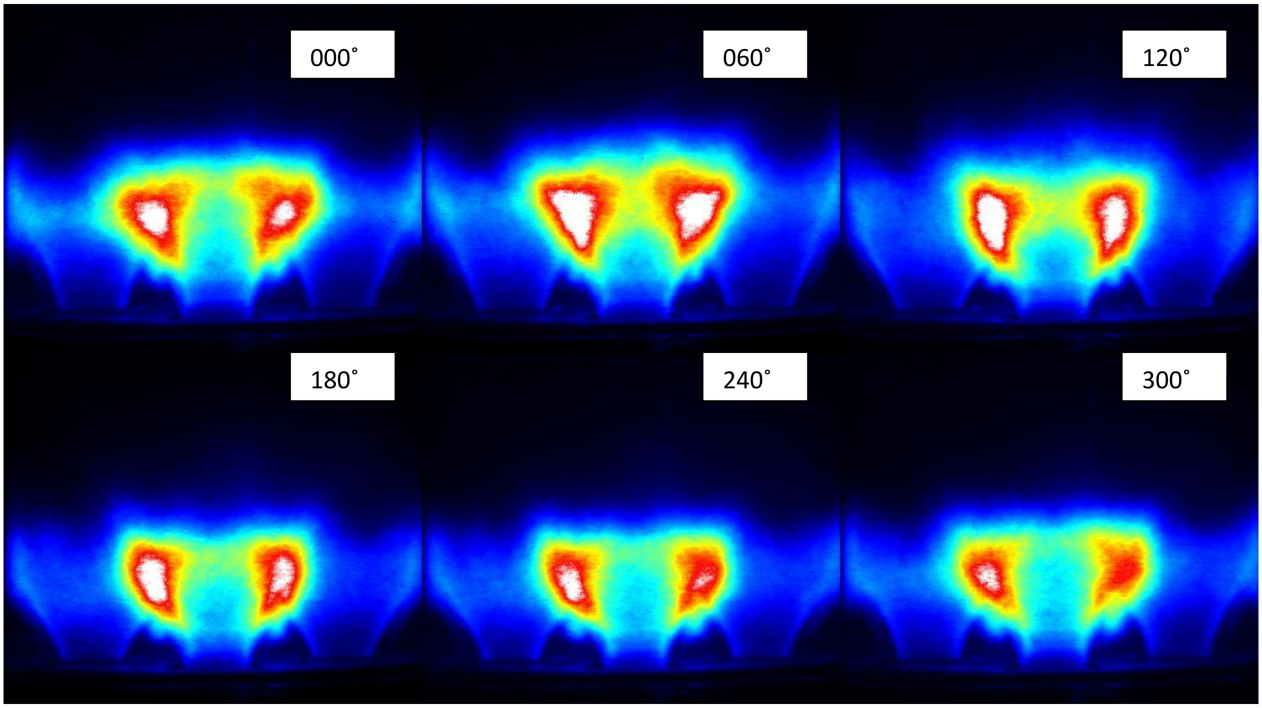

Figure 12: Phase Locked Image Set, u_{mean} = 20 m/s, T_{inlet} = 200C, Φ = .6, 125 hz forcing, u' = 5% , Phase displayed with respect to trigger signal

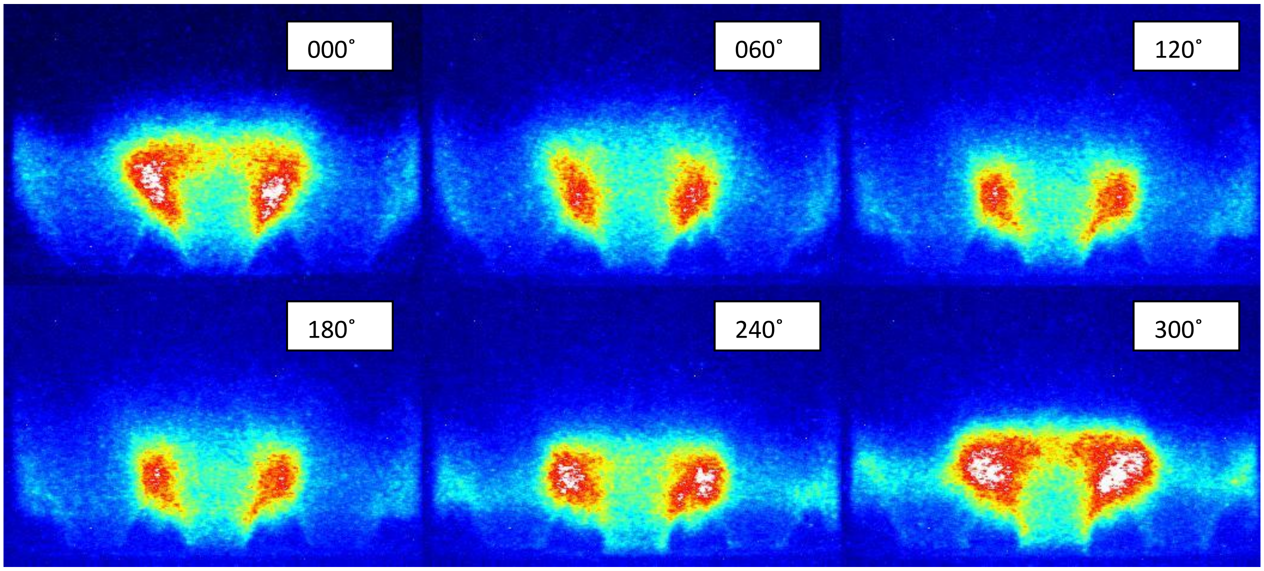

Figure 13: Phase locked image set, u_{mean} = 20 m/s, T_{inlet} = 200C, Φ = .6, 275 hz forcing, u' = 15%

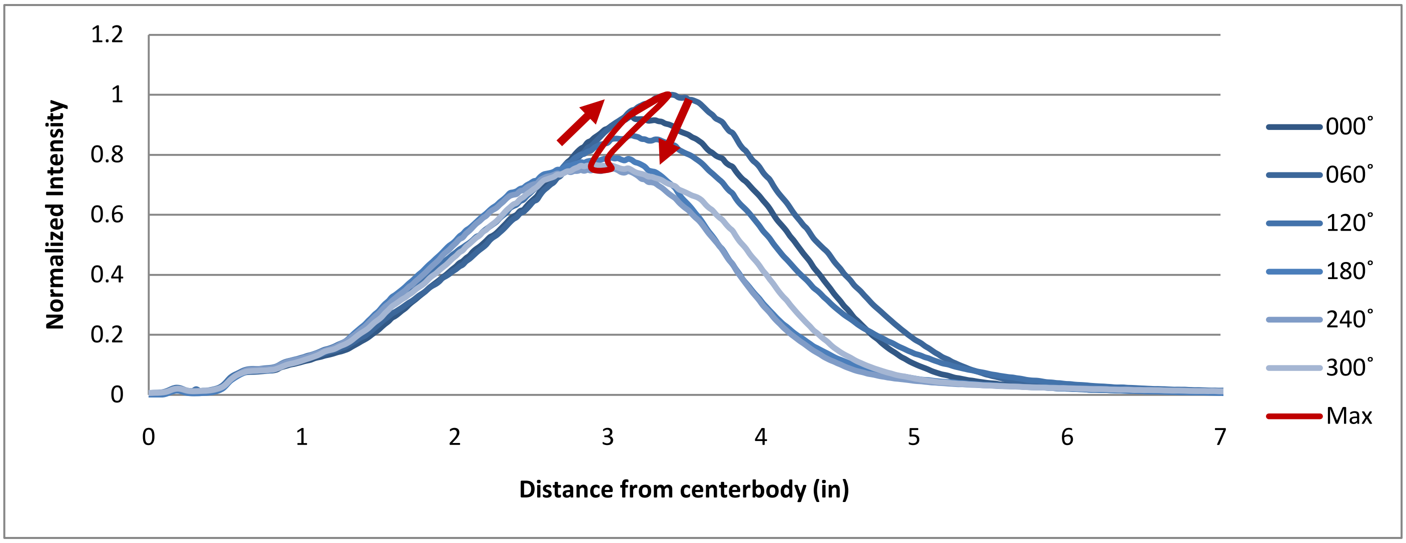

Figure 10: Axial Heat Release for a forced cycle, u_{mean} = 20 m/s, T_{inlet} = 200C, Φ = .6, 125 hz forcing, u' = 5%

CONCLUSION

The response of a multi-nozzle swirled lean premixed flame to inlet velocity perturbations has been measured for a fixed forcing amplitude. Several operating conditions match those run on a single-nozzle combustor with the same nozzle design and allow for comparisons between the two flame types.

The flame length is found to decrease with increasing inlet temperature or increasing equivalence ratio. As the velocity increases, the flame length increases but levels off. This could be evidence of increased flame interaction leading to increased burning rate.

By subjecting the combustor to a controlled velocity perturbation, a series of flame transfer functions were determined from 100 to 450 Hz for four different mean velocities. Across the forcing frequencies the gain transitions through a series of minima and maxima indicative of the constructive and destructive interference of two coupling mechanisms. For the multi-nozzle and single-nozzle flames the extrema occur at a similar frequency, suggesting that the mechanisms are the same for both configurations.

When plotted versus frequency, the FTFs at each mean velocity are qualitatively similar, but the frequencies at which the minimum and maximum gain occurs vary significantly. When plotted versus the non-dimensional Strouhal number, however, there is a degree of collapse. The first minimum occurs at nearly the same Strouhal number at all mean velocities. The maxima agree less, but there is still an improvement versus the frequency plots. This implies that the relative phase of the two perturbing mechanisms is largely controlled by the convective time scale, as evidenced by the Strouhal collapse.

The response of the multi-nozzle flame was found to be very similar to that of single-nozzle flames, except at the high and low ends of the range of forcing frequencies of interest. At low frequencies there is a decrease in gain between the single-nozzle flame and the multi-nozzle flame. At higher frequencies, while the pattern is similar, the multi-nozzle gain is slightly higher compared to the single-nozzle gain.

ACKNOWLEDGEMENT

The authors would like to acknowledge Mr. Larry Horner for fabricating many of the components of the multi-nozzle combustor. The material presented in this paper is based upon work supported by the Department of Energy National Energy Technology Laboratory under Award Number DE-NT0005054.

REFERENCES

[1] Ducruix, S., Schuller, T., Durox, D. and Candel, S., 2003, "Combustion Dynamics and Instabilities: Elementary Coupling and Driving Mechanisms," Journal of Propulsion and Power, **19,** pp. 722-733.

[2] Kim, K. T., Lee, J. G., Lee, H. J., Quay, B. D. and Santavicca, D. A., 2009, "Characterization of Forced Response of Swirl Stabilized Turbulent Lean-Premixed Flames in a Gas Turbine Combustor," Journal of Engineering for Gas Turbines and Power, **132,** pp. .

[3] Zinn, B. T. and Lieuwen, T. C., 2005, "Combustion Instabilities: Basic Concepts." In Combustion Instabilities in Gas Turbine Engines: Operational Experience, Fundamental Mechanisms and Modeling 3-24.

[4] Jones, B., Lee, J. G., Quay, B. D. and Santavicca, D. A., 2010, "Flame Response Mechanisms Due to Velocity Preturbations in a Lean Premixed Gas Turbine Combustor," Journal of Engineering for Gas Turbines and Power, **133,** pp. 1-9.

[5] Preetham, Thumuluru, S. K., Santosh, H. and Lieuwen, T. C., 2010, "Linear Response of Laminar Premixed Flames to Flow Oscillations: Unsteady Stretch Effects," Journal of Propulsion and Power, **26,** pp. 524-532.

[6] Lacarelle, A., Faustmann, T., Greenblatt, D., Paschereit, C. O., Lehmann, O., Luchtenburg, D. M. and Noack, B. R., 2009, "Spatiotemporal

Characterization of a Conical Swirler Flow Field under Strong Forcing," Journal of Engineering for Gas Turbines and Power, **131,** pp. .

[7] Valera-Medina, A., Syred, N. and Griffiths, A., 2009, "Visualization of Isothermal Large Coherent Structures in a Swirl Burner," Combustion and Flame, **156,** pp. 1723-1734.

[8] Renard, P. H., Thevenin, D., Rolon, J. C. and Candel, S., 2000, "Dynamics of Flame/Vortex Interactions," Progress in Energy and Combustion Science, **26,** pp. 225-282.

[9] Schadow, K. C. and Gutmark, E., 1991, "Combustion Instability Related to Vortex Shedding in Dump Combustors and Their Passive Control," Progress in Energy and Combustion Science, **18,** pp. 117-132.

[10] Palies, P., Durox, D., Schuller, T. and Candel, S., 2010, "The Combined Dynamics of Swirler and Turbulent Premixed Swirling Flames," Combustion and Flame, **157,** pp. 1698-1717 .

[11] Lieuwen, T. C. and McManus, K., 2003, "Introduction: Combustion Dynamics in Lean-Premixed Prevaporized (Lpp) Gas Turbines " Journal of Propulsion and Power, **19,** pp. 721.

[12] Kim, K. T., Lee, J. G., Quay, B. D. and Santavicca, D. A., 2010, "Response of Partially Premixed Flames to Acoustic Velocity and Equivalence Ratio Perturbations," Combustion and Flame, **157,** pp. 1731-1744.

[13] Rehm, J. E. and Clemens, T., 1998, "The Relationship between Vorticity/Strain and Reaction Zone Structure in Turbulent Non-Premixed Jet Flames," 27th International Symposium on Combustion.

[14] Nair, S. and Lieuwen, T., 2007, "Near Blowoff Dynamics of a Bluff Body Stabilized Flame," Journal of Propulsion and Power, **23,** pp. 421-427.

[15] Thumuluru, S. K., Ma, H.-H. and Lieuwen, T., 2007, "Measurements of the Flame Reponse to Exciation in a Swirl Combustor," AIAA2007-0845, 45th AIAA Aerospace Sciences Meeting and Exhibit, Reno, Nevada.

[16] Lieuwen, T. C. and Neumeier, Y., 2002, "Nonlinear Pressure-Heat Release Transfer Function Measurements in a Premixed Combustor," Proceedings of the Combustion Institute, **29,** pp. .

[17] Durox, D., Schuller, T., Noiray, N. and Candel, S., 2009, "Experimental Analysis of Nonlinear Flame Transfer Functions for Different Flame Geometries," Proceedings of the Combustion Institute, **132,** pp. 1391-1398.

[18] Merk, H. J., 1957, "An Analysis of Unstable Combustion of Premixed Gases," 6th International Symposium on Combustion.

[19] Kunze, K., Hirsch, C. and Sattelmayer, T., 2003, "Transfer Function Measurements on a Swirl Stabilized Premix Burner in an Annular Combustion Chamber," GT2004-53106, ASME Turbo Expo 2004, Vienna, Austria.

[20] Fanaca, D., Alemela, P. R., Hirsch, C. and Sattelmayer, T., 2010, "Comparison of the Flow Field of a Swirl Stabilized Premixed Burner in an Annular and a Single Burner Combustion Chamber," Journal of Engineering for Gas Turbines and Power, **132,** pp. 1-7.

[21] Staffelbach, G., Gicquel, L. Y. M., Boudier, G. and Poinsot, T., 2009, "Large Eddie Simulation of Self Excited Azimuthal Modes in Annular Combustors," Proceedings of the Combustion Institute, **32,** pp. 2909-2916.

[22] Fureby, C., 2010, "Les of a Multi-Burner Annular Gas Turbine Combustor," Flow Turbulence Combustion, **84,** pp. 543-564.

[23] Lee, J. G. and Santavicca, D. A., 2003, "Experimental Diagnostics for the Study of Combustion Instabilities in Premixed Combustors," Journal of Propulsion and Power, **19,** pp. 735-750.

[24] Waser, M. P. and Crocker, M. J., 1984, "Introduction to the Two-Microphone Cross-Spectral Density Method of Determining Sound Intensity," Noise Control Engineering, **22,** pp. 76-85.

[25] Figura, L., Lee, J. G., Quay, B. D. and Santavicca, D. A., 2007, "The Effects of Fuel Composition on Flame Structure and Combustion Dynamics in a Lean Premixed Combustor," GT2007-27298, ASME Turbo Expo 2007, Montreal, Canada .

[26] Turns, S. R. 1996. "An Introduction to Combustion: Concepts and Application." Boston, USA: McGraw Hill.

[27] Poinsot, T. and Veynante, D. 2005. "Theoretical and Numerical Combustion." Philadelphia, PA: Edwards.

[28] Boudy, F., Durox, D., Schuller, T., Jomaas, G. and Sebastien Candel, S., 2010, "Describing Function Analysis of Limit Cycles in a Multiple Flame Combustor," GT2010 - 22372, ASME Turbo Expo 2010, Glasgow, Scotland.